ARTICLE

Photoinduced Decomposition of Formaldehyde on Rutile TiO_2(100)-(1×1)†

Xiao Chen[a,b], Fang-liang Li[b,c], Qing Guo[a]*, Dong-xu Dai[a], Xue-ming Yang[a]*

a. State Key Laboratory of Molecular Reaction Dynamics, Dalian Institute of Chemical Physics, Chinese Academy of Science, Dalian 116023, China
b. University of Chinese Academy of Sciences, Beijing 100049, China
c. School of Physical Science and Technology, ShanghaiTech University, Shanghai 201210, China

(Dated: Received on June 8, 2018; Accepted on June 25, 2018)

We have investigated the photoinduced decomposition of formaldehyde (CH_2O) on a rutile TiO_2(100)-(1×1) surface at 355 nm using temperature-programmed desorption. Products, formate ($HCOO^-$), methyl radical (CH_3·), ethylene (C_2H_4), and methanol (CH_3OH) have been detected. The initial step in the decomposition of CH_2O on the rutile TiO_2(100)-(1×1) surface is the formation of a dioxymethylene intermediate in which the carbonyl O atom of CH_2O is bound to a Ti atom at the five-fold-coordinated Ti^{4+} (Ti_{5c}) site and its carbonyl C atom bound to a nearby bridge-bonded oxygen (O_b) atom, respectively. During 355 nm irradiation, the dioxymethylene intermediate can transfer an H atom to the O_b atom, thus forming $HCOO^-$ directly, which is considered as the main reaction channel. In addition, the dioxymethylene intermediate can also transfer methylene to the O_b row and break the C−O bond, thus leaving the original carbonyl O atom at the Ti_{5c} site. After the transfer of methylene, several pathways to products are available. Thus, we have found that O_b atoms are intimately involved in the photoinduced decomposition of CH_2O on the rutile TiO_2(100)-(1×1) surface.

Key words: Rutile TiO_2(100)-(1×1), Formaldehyde, Temperature-programmed desorption, Photoinduced decomposition

I. INTRODUCTION

Titanium dioxide (TiO_2), is one of the most important metal oxides used in catalysis and photocatalysis [1–5]. Formaldehyde (CH_2O) is a key species (reagent, intermediate, or product) in various catalytic and photocatalytic reactions, such as methanol (CH_3OH) synthesis [6–8], CH_3OH oxidation [9–13], and hydrocarbon production [14, 15]. In addition, CH_2O is one of the main indoor air pollutions in our daily life. It has been reported that TiO_2-based catalysts are widely used in thermally catalytic and photocatalytic reactions involving CH_2O. Therefore, it is of significant importance to gain an insightful understanding of the interactions of CH_2O with TiO_2 surfaces.

The adsorption and reactions of CH_2O on TiO_2 surfaces have been extensively studied both experimentally and theoretically [16–29]. It has been well-established that CH_2O can adsorb on TiO_2 surfaces in two different configurations [19, 21–23, 25, 28, 29]. First, CH_2O can weakly adsorb at a surface 5-fold-coordinated Ti^{4+} (Ti_{5c}) site in a monodentate configuration (η^1-CH_2O), where it binds weakly via its O atom to the surface Ti_{5c} atom. Alternatively, it can also adsorb in a bidentate fashion (η^2-CH_2O), where it binds to the surface strongly with its O atom bound to a surface Ti_{5c} atom, and its C atom bound to an adjacent bridging oxygen (O_b) atom. When TiO_2 surfaces contain bridging oxygen vacancy (O_v) sites, CH_2O can adsorb at O_v sites [20, 23, 29]. Further heating may result in the formation of other products via the carbon-carbon coupling reactions of two CH_2O molecules, such as ethylene (C_2H_4) [19, 21–23, 29]. In addition, the possibility of forming paraformaldehyde chains on rutile TiO_2(110) has also been reported by Wöll and coworkers [25, 30].

The photochemistry of CH_2O has also been investigated extensively on various TiO_2 surfaces and formate ($HCOO^-$) is observed as a main product [17–19, 27, 29, 31]. On rutile TiO_2(110), Xu and coworkers found that the photoinduced decomposition of CH_2O could occur efficiently to produce $HCOO^-$, methyl radical (CH_3·) and C_2H_4 in the absence of surface oxygen species [17]. It was proposed that although lattice oxygen atoms may not appear in $HCOO^-$ product, they are intimately involved in the photoinduced decomposition of CH_2O on rutile TiO_2(110). Later, Cremer and coworkers reported that the formation of $HCOO^-$ is the dominate reaction channel and the efficiency of $HCOO^-$

†Part of the special issue for celebration of "the 60th Anniversary of University of Science and Technology of China and the 30th Anniversary of Chinese Journal of Chemical Physics".
*Authors to whom correspondence should be addressed.
E-mail: guoqing@dicp.ac.cn, xmyang@dicp.ac.cn

formation on rutile TiO_2(110) with surface oxygen species is about 4 times larger than that without surface oxygen species [18]. On the reduced anatase TiO_2(001)-(1×4) [27] and rutile TiO_2(011)- (2×1) surfaces [29], the photolysis of CH_2O also produces $HCOO^-$ as the main product in the absence of surface oxygen species. The rutile TiO_2(100)-(1×1) surface is one of the common facets of rutile TiO_2, but the photochemistry of CH_2O on the rutile TiO_2(100)-(1×1) surface has not been reported and an insightful understanding of photocatalytic reactions of CH_2O on the rutile TiO_2(100)-(1×1) surface is thus lacking. In this work, we have investigated the photocatalytic reactions of CH_2O on the rutile TiO_2(100)-(1×1) surface at 355 nm with temperature-programmed desorption (TPD) method. Without irradiation, nearly no thermal reaction products are observed. Under UV irradiation, CH_2O is mainly decomposed into $HCOO^-$. While, CH_3OH, CH_3·, and C_2H_4 are detected as minor products at elevated temperature during the TPD process. These results will help broaden the fundamental understandings of CH_2O photochemistry on TiO_2 surfaces.

II. EXPERIMENTAL METHODS

TPD experiments were carried out in an ultra-high vacuum (UHV) chamber with a base pressure of 6×10^{-11} Torr. Details of this TPD apparatus have been described elsewhere [10]. TPD signals were detected by a quadrupole mass spectrometer (Extrel). The third harmonic (355 nm) output of a diode pumped, solid state, Q-switched 1064 nm laser (Spectra-Physics) was used as the UV light resource for the photocatalytic reactions of CH_2O in our experiments. The laser was operated with a pulse time of 12 ns and a repetition rate of 50 kHz. The average power of the light used in our experiments was approximately 20 mW, corresponding to $\sim6.5\times10^{16}$ photons/(cm^2·s).

The rutile TiO_2(100) single crystal was purchased from Princeton Scientific Corp., with a size of 10 mm×10 mm×1 mm. The surface was cleaned by repeated cycles of Ar^+ sputtering and annealing in $>4\times10^{-7}$ Torr O_2 at 800 K. Then the ordering and cleanness of the sample were confirmed by a sharp (1×1) low energy electron diffusion (LEED) pattern and Auger electron spectroscopy (AES), respectively. CH_2O was obtained via the thermal decomposition of paraformaldehyde (95% purity, Sigma-Aldrich). Prior to experiments, the purity of CH_2O was checked by our spectrometer. The purified CH_2O was introduced into the surface through a calibrated molecular beam doser at about 120 K. TPD spectra were measured with a ramping rate of 2 K/s, and with the surface facing the mass spectrometer.

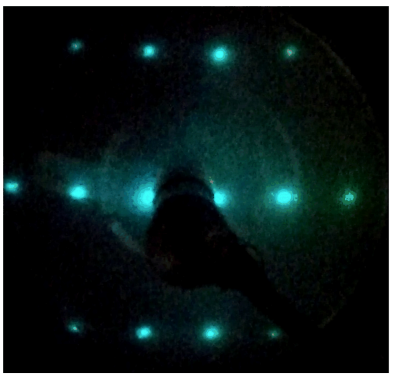

FIG. 1 The LEED (low energy electron diffraction) pattern for the rutile TiO_2(100)-(1×1) surface at E_{el}=50 eV after the surface cleaning process was accomplished.

III. RESULTS

A. The adsorption and reactions of CH_2O on the rutile TiO_2(100)-(1×1) surface

Before TPD experiments, the surface condition was checked by LEED and water (H_2O) TPD spectra, respectively. As shown in FIG. 1, a sharp (1×1) LEED pattern for the rutile TiO_2(100)-(1×1) surface is observed, which confirms the ordering of the surface. To further confirm the surface condition, TPD spectra of H_2O at different coverages were subsequently collected. At the highest H_2O coverage (4 ML, 1 ML=7.36×10^{14} molecules/cm^2), four main desorption features at 147, 167, 242, and 300 K are detected in our TPD spectra (FIG. 2), which is similar to previous results of H_2O on the rutile TiO_2(100)-(1×1) surface [32, 33], indicating that a well-defined and unreconstructed (1×1) surface has been obtained. On the basis of previous studies [32, 33], the 147, 167, 242, and 300 K peaks are due to desorption of H_2O from multilayer (ice layer), second layer, molecular adsorption at Ti_{5c} sites, and dissociative adsorption at Ti_{5c} sites, respectively. Whereas, no desorption peak at higher temperature is detected, implying that no surface O_v sites exist on the surface.

Afterwards, we carried out experiments with CH_2O adsorption on the rutile TiO_2(100)-(1×1) surface. As shown in FIG. 3, TPD spectra were collected at a mass-to-charge ratio (m/z) of 30 (CH_2O^+) after rutile TiO_2(100)-(1×1) surfaces were dosed with different coverages of CH_2O. At low coverages (<0.26 ML), a single desorption peak appears at ~310 K and increases in intensity with increasing CH_2O coverage, and its peak position nearly keeps unchanged. When the CH_2O coverage is higher than 0.26 ML, an additional desorption peak appears at around 260 K. As CH_2O coverage increases, the intensity of the 260 K peak increases, with its peak position shifting to lower temperature until 255 K. Although the 310 K peak is seriously overlapped

DOI:10.1063/1674-0068/31/cjcp1806137

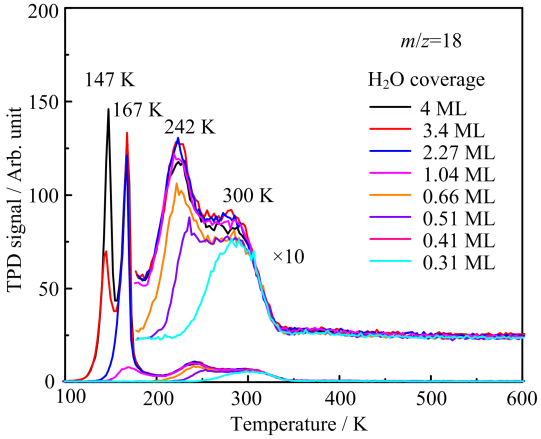

FIG. 2 Typical spectra collected at mass-to-charge (m/z) of 18 (H_2O^+) after the rutile TiO_2(100)-(1×1) surfaces were dosed with various coverages of H_2O at 120 K.

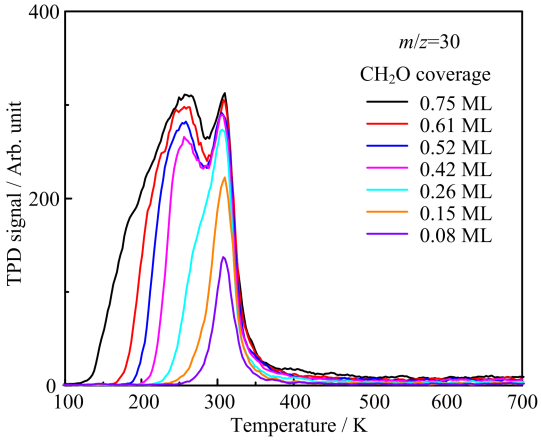

FIG. 3 Typical spectra collected at mass-to-charge (m/z) of 30 (CH_2O^+) after the rutile TiO_2(100)-(1×1) surfaces were dosed with various coverages of CH_2O at 120 K.

with the 260 K peak, the occurrence of two desorption peaks shows the possibility of two different CH_2O adsorption configurations on the rutile TiO_2(100)-(1×1) surface. Since the lowest surface temperature that we could achieve in this work is 120 K, the highest coverage of CH_2O on the rutile TiO_2(100)-(1×1) surface is about 0.75 ML.

Based on previous TPD results of CH_2O on rutile TiO_2(110) [17], the desorption of η^1-CH_2O gives a TPD peak at 280 K. Theoretical calculations [19, 20, 23–25] predict that the η^1 configuration of CH_2O has an adsorption energy of ∼0.7 eV, and the η^2 configuration has an adsorption energy of ∼1.3 eV. CH_2O may also adsorb at O_v sites with an adsorption energy of about 0.89−0.99 eV. Thus, η^2-CH_2O is the more stable adsorption configuration. However, only the η^1 configuration of CH_2O can be formed on rutile TiO_2(110) after adsorption, and the transition from the η^1 configuration to the η^2 configuration requires a long time

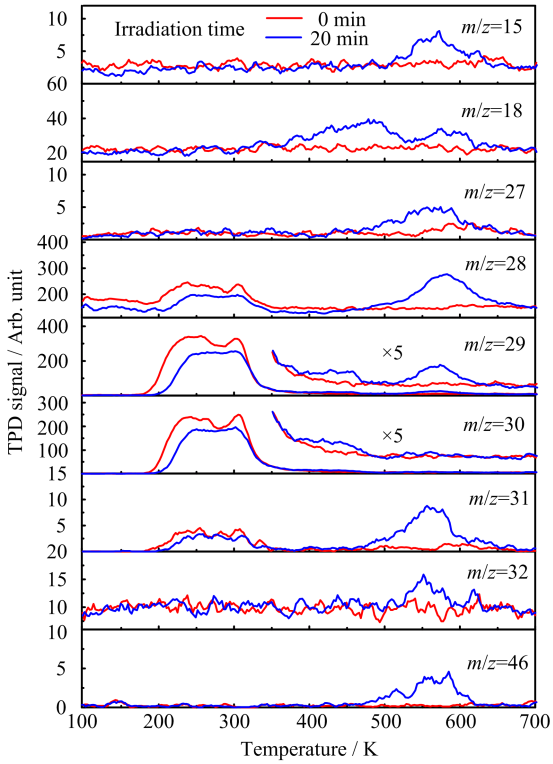

FIG. 4 The rutile TiO_2(100)-(1×1) surfaces were dosed with 0.52 ML of CH_2O at 120 K. Typical TPD spectra collected at m/z=15 (CH_3^+), 18 (H_2O^+), 27 ($C_2H_3^+$), 28 ($C_2H_4^+$, CO^+), 29 (HCO^+), 30 (CH_2O^+), 31(CH_2OH^+), 32 (CH_3OH^+), and 46 ($HCOOH^+$) following 0 min (red lines) and 20 min (blue lines) irradiation.

[23]. In this work, the rutile TiO_2(100)-(1×1) surface contains no O_v sites, and thus CH_2O can only adsorb at Ti_{5c} sites. As shown in the CH_2O TPD spectra (FIG. 3), the peak position of the 310 K peak is only about 55 K higher than that of the 255 K peak. According to the first-order thermal desorption model (with a typical pre-exponential factor value of 10^{13}/s) [34], the difference between desorption energies of these two peaks is less than 0.2 eV. Therefore, the 310 and 255 K peaks could not be due to desorption of η^2-CH_2O and η^1-CH_2O, respectively. Conversely, the two desorption peaks may be due to desorption of η^1-CH_2O at Ti_{5c} sites. Because the population of Ti_{5c} sites on the rutile TiO_2(100)-(1×1) surface is about 1.5 times bigger than that on rutile TiO_2(110), the repulsive interaction between CH_2O molecules adsorbed at Ti_{5c} sites on the rutile TiO_2(100)-(1×1) surface will be much stronger than that on rutile TiO_2(110). In this case, the appearance of the 255 K peak is likely the result of the strong intermolecular repulsions between CH_2O molecules adsorbed at Ti_{5c} sites.

In addition to desorbed parent CH_2O, other possible desorption products were examined by comprehensively monitoring various signals of m/z=15, 18, 27, 28, 29, 30, 31, 32, and 46 (FIG. 4). No evidence of other re-

DOI:10.1063/1674-0068/31/cjcp1806137

action products was found. The phenomenon is also observed on anatase TiO_2(101) [28]. But it is considerably different from the phenomenon observed on rutile TiO_2(110) [19, 21, 22], rutile TiO_2(100)-(2×1) [29], and the reduced anatase TiO_2(100)-(1×4) surfaces [27]. On these surfaces [19, 21, 22, 27, 29], two CH_2O molecules can be coupled to form C_2H_4, and surface O_v sites are identified as the reactive sites for the formation of C_2H_4. In our experiments, the rutile TiO_2(100)-(1×1) surface used is annealed in $>4\times10^{-7}$ Torr O_2, and nearly no surface O_v sites exist on the rutile TiO_2(100)-(1×1) surface after sample preparation. Therefore, it is reasonable that no thermal products are detected after CH_2O adsorption.

B. The photocatalytic reactions of CH_2O on the rutile TiO_2(100)-(1×1) surface

FIG. 5 shows TPD spectra acquired at mass-to-charge ratios (m/z) of 28 (CO^+, $C_2H_4{}^+$), and 30 (CH_2O^+) after rutile TiO_2(100)-(1×1) surfaces were dosed with 0.52 ML of CH_2O and then irradiated by a laser at 355 nm for various durations. Before irradiation, the signal profiles of the 260 K peak and the 310 K peak from m/z=28 are exactly same as those from m/z=30, suggesting that both peaks are the results of dissociative ionization of desorbed parent CH_2O molecules in the electron-bombardment ionizer. As mentioned above, no other reaction products are detected, implying that this surface is thermally inactive for the reactions of CH_2O.

After UV irradiation, both CH_2O peaks at 260 and 310 K decrease monotonically as the laser irradiation time increases, suggesting that CH_2O molecules are either photo-desorbed or reacted to form other products. A TPD peak at ~440 K becomes obvious in the TPD trace of m/z=30 after irradiation and keeps nearly unchanged with increasing irradiation time (FIG. 5(a)). Taking into account additional traces of m/z=29 (FIG. 4), this peak is also assigned to desorption of CH_2O. This result suggests that part of CH_2O molecules have become more strongly bound to the surface after irradiation. A similar phenomenon has been observed on rutile TiO_2(110) [17], which may be due to the formation of η^2-CH_2O after irradiation.

$$CH_2O_{Ti5c}+O_b\rightarrow O_b\text{-}CH_2\text{-}O_{Ti5c} \quad (1)$$

In our work, the 440 K peak is also likely due to the formation of η^2-CH_2O. Based on previous work of aldehydes photochemistry on rutile TiO_2(110) [35], the O_{Ti5c}-CH_2-O_b species is very photoactive, and can be easily decomposed into $HCOO^-$. As a result, the amount of η^2-CH_2O on the surface will not keep increasing with increasing irradiation time.

Concomitant to the decrease in the CH_2O TPD peaks, the TPD signal for m/z=28 at around 580 K increases with increasing irradiation time (FIG. 5(b)).

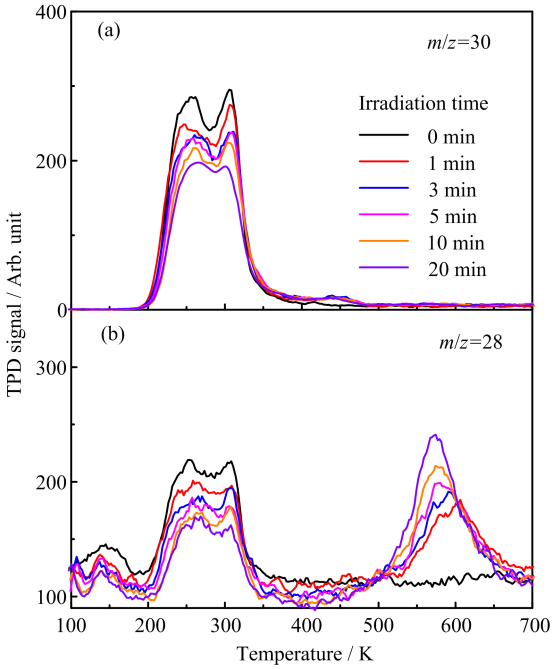

FIG. 5 The rutile TiO_2(100)-(1×1) surfaces were dosed with 0.52 ML of CH_2O at 120 K. (a) Typical TPD spectra collected at m/z=30 (CH_2O^+) following different laser irradiation times. (b) Typical TPD spectra collected at m/z=28 ($C_2H_4{}^+$, CO^+) following different laser irradiation times.

Considering the small adsorption energy of CO on the surface, the 580 K peak could only come from the thermal decomposition of other species. In order to determine the origin of this new feature, TPD traces were collected at a variety of m/z ratios (FIG. 4). On the basis of the TPD results in FIG. 4, the m/z=28 signal at 580 K may come from three sources. Compared with previous results of HCOOH on rutile TiO_2(100) [36] and the cracking patterns of HCOOH observed in our mass spectrometer, the first two sources of m/z=28 signal at 580 K are HCOOH and $HCOO^-$, both of which could be the products of CH_2O photo-oxidation.

The large TPD signal seen in FIG. 5(b) indicates that $HCOO^-$ may be an important photoinduced product. Compared to other products, the intensity of the 580 K peak is several times greater (see FIG. 4), strongly suggesting that $HCOO^-$ is probably the major product of the photoinduced decomposition of CH_2O on the rutile TiO_2(100)-(1×1) surface. The yields of CO (from $HCOO^-$) and CH_2O with increasing irradiation time are calculated and displayed in FIG. 6. About 0.19 ML of CH_2O is depleted after 20 min irradiation, whereas, only 0.023 ML of $HCOO^-$ is produced, implying that the decrease of the CH_2O signal is mainly the result of photoinduced desorption of CH_2O during laser irradiation.

In order to produce $HCOO^-$, the C atom of the CH_2O molecule must acquire a second O atom. According to previous work [17], without additional sur-

DOI:10.1063/1674-0068/31/cjcp1806137

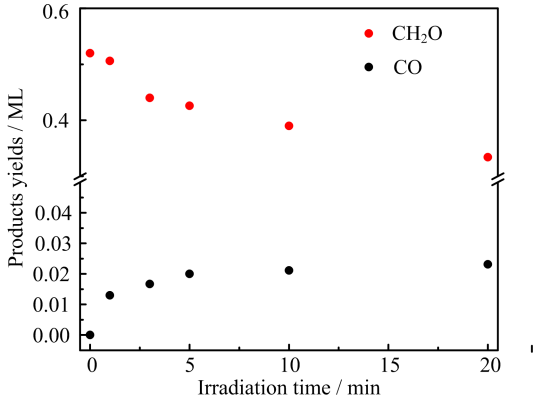

FIG. 6 Yields of CH_2O and CO as a function of laser irradiation time following the adsorption of 0.52 ML of CH_2O on the rutile TiO_2(100)-(1×1) surfaces at 120 K, derived from data in FIG. 5.

face oxygen species, the second O atom is either from an O_b row or from another adsorbed CH_2O molecule. The direct photodissociation of CH_2O to produce an O atom via the C=O bond cleavage is not possible because of the extremely low adsorption cross section of CH_2O at 355 nm ($\sim 10^{-20}$ cm^2) [37]. Xu and coworkers [17] proposed that an O atom at the Ti_{5c} site (O_{Ti5c}) can be produced via the transfer of methylene from CH_2O to an O_b atom during UV irradiation through an intermediate adsorption structure consisting of dioxymethylene.

$$O_b\text{-}CH_2\text{-}O_{Ti5c} \rightarrow O_b\text{-}CH_2 + O_{Ti5c} \quad (2)$$

Subsequently, the O_{Ti5c} atom may react with a nearby adsorbed CH_2O molecule to form an O_{Ti5c}-CH_2-O_{Ti5c} complex by heat or laser irradiation.

$$O_{Ti5c} + CH_2O_{Ti5c} \rightarrow O_{Ti5c}\text{-}CH_2\text{-}O_{Ti5c} \quad (3)$$

Then the complex perhaps gives rise to $HCOO^-$ either by transferring an H atom to an O_b atom (HO_b), or ejecting an H atom to the vacuum.

$$O_{Ti5c}\text{-}CH_2\text{-}O_{Ti5c} + O_b \rightarrow HCOO_{Ti5c}{}^- + HO_b \quad (4)$$
$$O_{Ti5c}\text{-}CH_2\text{-}O_{Ti5c} \rightarrow HCOO_{Ti5c}{}^- + H \quad (5)$$

In addition, $HCOO_{Ti5c}{}^-$ may combine with HO_b to produce HCOOH.

$$HCOO_{Ti5c}{}^- + HO_b \rightarrow HCOOH + O_b \quad (6)$$

While, as shown in TPD trace of m/z=18 (FIG. 4), two main desorption features at 478 and 580 K are observed after irradiating the 0.52 ML CH_2O covered rutile TiO_2(100)-(1×1) surface for 20 min. The 580 K peak may come from thermal decomposition of HCOOH and $HCOO^-$ [36]. For the 478 K peak, no signals of higher m/z ratios are detected at this temperature. Thus, this peak can be only due to the H_2O desorption. However, the desorption temperature is much higher than that of H_2O adsorbed at the Ti_{5c} sites of rutile TiO_2(100)-(1×1), and is similar to that of the recombinative desorption of H_2O from hydroxyls on O_b rows of rutile TiO_2(110) [38]. Thus, the 478 K peak is also likely from recombinative desorption of H_2O.

$$2HO_b \rightarrow H_2O + O_v \quad (7)$$

The formation of H_2O via the reaction (7) verifies that the reaction channel involving a dioxymethylene intermediate is very possible to proceed on the surface, resulting in the formation of $HCOO^-$ eventually.

The reaction channel consisting of a dioxymethylene intermediate is also supported by the observation of other products. As shown in FIG. 7(a), typical TPD spectra of m/z=27 ($C_2H_3{}^+$) were collected after irradiating the 0.52 ML CH_2O covered rutile TiO_2(100)-(1×1) surfaces for different time with a laser at 355 nm. Before irradiation, no signal is observed. As irradiation time increases, a peak at ~580 K appears and increases in intensity. Based on previous works [17, 19, 21, 22], this peak is due to desorption of C_2H_4 product, which is formed via the carbon-carbon coupling of two CH_2O moleules. Clearly, C_2H_4 product is another source for the m/z=28 signal at 580 K. This is very similar to the observation of CH_2O photodecomposition on the rutile TiO_2(110) surface. On rutile TiO_2(110), the C_2H_4 product arises from CH_2O adsorbed at O_v sites to form a diolate (-OCH_2CH_2O-) species, which releases C_2H_4 at a relatively high temperature [21, 22]. But the rutile TiO_2(100)-(1×1) surface used in our work contains no O_v sites. Thus, the dioxymethylene species may act as the intermediate for the formation of C_2H_4. After the transfer of methylene to O_b atoms, two O_b-CH_2 groups may be coupled to form C_2H_4.

$$2O_b\text{-}CH_2 \rightarrow C_2H_4 + 2O_b \quad (8)$$

While, another desorption peak appears at 570 K in the TPD spectrum of m/z=15 ($CH_3{}^+$) after UV irradiation and increases with irradiation time (FIG. 7(b)). This peak is attributed to CH_3 radical desorption, probably from O_b atoms. The formation of CH_3O_b may also need the participation of O_b-CH_2 groups.

$$O_b\text{-}CH_2 + HO_b \rightarrow O_b\text{-}CH_3 + O_b \quad (9)$$
$$O_b\text{-}CH_3 \rightarrow CH_3\cdot + O_b \quad (10)$$

The appearance and increase of $CH_3\cdot$ on O_b atoms further demonstrate that methylene groups can be transferred to O_b atoms during irradiation. Therefore, it can be concluded that the reaction channel involving the dioxymethylene intermediate is very likely to proceed on the rutile TiO_2(100)-(1×1) surface.

It is also noteworthy that the intensity of CO signal at 580 K is about 20 times bigger than that of C_2H_4 signal, and about 40 times bigger than that of $CH_3\cdot$ signal after 20 min irradiation (see FIG. 5 and FIG. 7).

DOI:10.1063/1674-0068/31/cjcp1806137

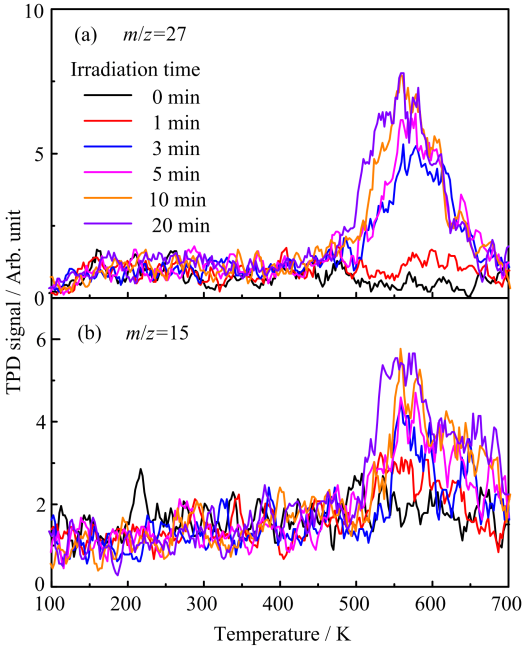

FIG. 7 The rutile $TiO_2(100)$-(1×1) surfaces were dosed with 0.52 ML of CH_2O at 120 K. (A) Typical TPD spectra collected at m/z=27 ($C_2H_3^+$) following different laser irradiation times. (B) Typical TPD spectra collected at m/z=15 (CH_3^+) following different laser irradiation time.

These results suggest that the dominant photocatalytic reaction is the formation of $HCOO^-$. Meanwhile, at the first 1 min irradiation, nearly no C_2H_4 and CH_3· products are formed (FIG. 7), but the $HCOO^-$ product has been largely formed (bigger CO desorption signal in FIG. 5(b)). In other words, the formations of C_2H_4 and CH_3· are not exactly coincident with the formation of $HCOO^-$ and the formation of $HCOO^-$ precedes the formations of C_2H_4 and CH_3·. As a result, the formation of $HCOO^-$ may not completely depend on the formation of the O_{Ti5c} atoms. On the contrary, the O_b-CH_2-O_{Ti5c} intermediate is likely to decompose into $HCOO^-$ directly, transferring an H atom to the nearby O_b atom (HO_b).

$$O_b\text{-}CH_2\text{-}O_{Ti5c}+O_b \rightarrow HCO_bO_{Ti5c}^- + HO_b \qquad (11)$$

In addition to the increase in the m/z=28 signal at around 580 K, a new desorption peak appears at about 570 K in the TPD trace of m/z=31 (FIG. 8) and increases with increasing irradiation time. Taking into account additional TPD traces in FIG. 4, this peak is attributed to desorption of CH_3OH. This phenomenon has been observed previously on rutile $TiO_2(110)$ [19] and the reduced anatase $TiO_2(100)$-(1×4) surface [27]. In Huang's experiment [19], they proposed that the occurrence of H-transfer between $HCOO^-$ and dioxymethylene led to the formation of methoxy species (CH_3O). The disproportionation reaction between CH_3O could lead to the formation of

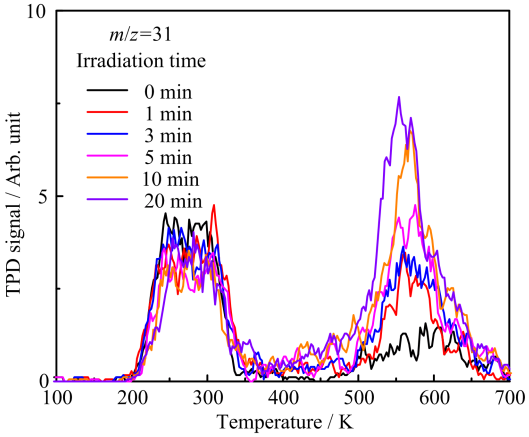

FIG. 8 Typical TPD spectra collected at m/z=31 (CH_2OH^+) after the rutile $TiO_2(100)$-(1×1) surfaces were dosed with 0.52 ML of CH_2O following different laser irradiation time.

CH_3OH and CH_2O at elevated temperature. Previous results of CH_2O on rutile $TiO_2(001)$ also show that the coincident desorption of CH_3OH and CH_2O could occur at 370 and 550 K, respectively [16]. However, we did not observe the coincident desorption of CH_3OH and CH_2O at 570 K. Based on previous work on rutile $TiO_2(110)$ [39], CH_2O can recombine with HO_b to form CH_3OH again. On the reduced anatase $TiO_2(100)$-(1×4) surface [27], Wang and coworkers also ascribed the formation of CH_3OH to the reaction of CH_2O with the produced H atoms during irradiation or during the heating process. Thus, on the rutile $TiO_2(100)$-(1×1) surface, the formation of CH_3OH may proceed as follows:

$$CH_2O_{Ti5c}+HO_b \rightarrow O_{Ti5c}\text{-}CH_3+O_b \qquad (12)$$

$$O_{Ti5c}\text{-}CH_3+HO_b \rightarrow CH_3OH \qquad (13)$$

While, during the TPD process, CH_3O_{Ti5c} may also decompose into CH_3· and O_{Ti5c}.

$$O_{Ti5c}\text{-}CH_3 \rightarrow CH_3\cdot + O_{Ti5c} \qquad (14)$$

IV. DISCUSSION

Although CH_2O is a very simple molecule, the photolysis of this molecule is very complicated. The products and reaction channels for CH_2O decomposition on different TiO_2 surfaces [19, 21, 22, 27, 29] are very similar. For rutile $TiO_2(100)$-(1×1) and anatase $TiO_2(101)$ surfaces [28], however, no other thermal reaction products were detected during the TPD process due to the absence of O_v sites on the surfaces. This result is also an evidence that O_v sites are the reactive sites for the carbon-carbon coupling of CH_2O to C_2H_4. Among all these TiO_2 surfaces discussed above, the desorption temperature of CH_2O is the highest on the rutile

DOI:10.1063/1674-0068/31/cjcp1806137

TiO_2(100)-(1×1) surface. That may be due to the fact that the densities of Ti_{5c} and O_b atoms on the rutile TiO_2(100)-(1×1) surface are much higher than those on the other TiO_2 surfaces. As a result, the carbonyl C atom of the CH_2O molecule may interact with the O_b atom more easily, which may result in the formation of a more stable adsorption configuration.

The rutile TiO_2(100)-(1×1) surface is thermally inactive for the reactions of CH_2O, but it is photoactive for the reactions of CH_2O. The main decomposition product is $HCOO^-$, which is similar to the results obtained on other TiO_2 surfaces [17, 19, 27, 29]. However, the dominant reaction channels leading to $HCOO^-$ formation may be different. On the rutile TiO_2(110) surface, the dominant reaction channel is consisted of the O_{Ti5c} atoms formation via the transfer of methylene to the O_b sites and the O_b-CH_2-O_{Ti5c} species acts as the intermediate [17]. Whereas, on the rutile TiO_2(100)-(1×1) surface, the case is very different. As shown in FIG. 5 and FIG. 7, the intensity of CO signal at 580 K is about 20 times bigger than that of C_2H_4 signal, and about 40 times bigger than that of CH_3· signal. These values are much bigger than the ratios of those produced from CH_2O photoinduced decomposition on rutile TiO_2(110) [17]. As mentioned above, the formations of C_2H_4 and CH_3· require the transfer of methylene to the O_b sites forming O_bCH_2. After the transfer process, the O_{Ti5c} atoms are produced simultaneously, which will take part in the following formation of $HCOO^-$. Whereas, the formation of $HCOO^-$ precedes the formation of C_2H_4 and CH_3· in this work. These results clearly indicate that O_{Ti5c} is probably not necessary for the formation of $HCOO^-$. Therefore, the dominant reaction channel on the rutile TiO_2(100)-(1×1) surface may be changed. The direct decomposition of O_b-CH_2-O_{Ti5c} into $HCO_bO_{Ti5c}{}^-$ and HO_b becomes the main reaction channel, while the reaction of O_{Ti5c} with CH_2O adsorbed at Ti_{5c} sites to produce $HCOO^-$ becomes a minor reaction channel. Therefore, on the rutile TiO_2(100)-(1×1) surface, two possible reaction channels may lead to the formation of $HCOO^-$ and the O_b-CH_2-O_{Ti5c} species maybe acts as the intermediate. The direct decomposition is considered as the dominant reaction channel and the lattice oxygen atom (O_b) is directly involved in the photoinduced decomposition of CH_2O on the rutile TiO_2(100)-(1×1) surface.

V. CONCLUSION

In this work, we have investigated the interactions of CH_2O with a rutile TiO_2(100)-(1×1) surface under UV irradiation. Experimental results show that the photodecomposition of CH_2O on the rutile TiO_2(100)-(1×1) surface can occur easily under UV light irradiation. Before irradiation, only molecular desorption of CH_2O can be detected during the TPD process. When irradiated by UV light, several photoinduced products are detected. $HCOO^-$ is the major product, while C_2H_4, CH_3·, and CH_3OH are minor products.

Our TPD investigation demonstrates that O_b atoms play a very important role in the photoinduced decomposition of CH_2O on the rutile TiO_2(100)-(1×1) surface through an initial O_b-CH_2-O_{Ti5c} intermediate structure. Clear mechanisms have been delineated for the participation of lattice (O_b) atoms in the decomposition pathways, including their presence in one type of $HCOO^-$ product. Our results are supposed to broaden the fundamental understanding of CH_2O photochemistry on TiO_2 surfaces.

VI. ACKNOWLEDGMENTS

This work was supported by the National Natural Science Foundation of China (No.21673235 and No.21403224), and the Youth Innovation Promotion Association CAS, and the Key Research Program of the Chinese Academy of Sciences.

[1] A. L. Linsebigler, G. Q. Lu, and J. T. Yates, Chem. Rev. **95**, 735 (1995).
[2] U. Diebold, Surf. Sci. Rep. **48**, 53 (2003).
[3] A. Fujishima, X. Zhang, and D. Tryk, Surf. Sci. Rep. **63**, 515 (2008).
[4] M. A. Henderson, Surf. Sci. Rep. **66**, 185 (2011).
[5] Q. Guo, C. Y. Zhou, Z. B. Ma, Z. F. Ren, H. J. Fan, and X. M. Yang, Chem. Soc. Rev. **45**, 3701 (2016).
[6] K. Klier, Adv. Catal. **31**, 243 (1982).
[7] M. Kurtz, J. Strunk, O. Hinrichsen, M. Muhler, K. Fink, B. Meyer, and C. Wöll, Angew. Chem. Int. Ed. **44**, 2790 (2005).
[8] M. Behrens, F. Studt, I. Kasatkin, S. Kuhl, M. Havecker, F. Abild-Pedersen, S. Zander, F. Girgsdies, P. Kurr, B. L. Kniep, M. Tovar, R. W. Fischer, J. K. Norskov, and R. Schlogl, Science **336**, 893 (2012).
[9] M. F. Camellone, J. Zhao, L. Jin, Y. Wang, M. Muhler, and D. Marx, Angew. Chem. Int. Ed. **52**, 5780 (2013).
[10] Q. Guo, C. B. Xu, Z. F. Ren, W. S. Yang, Z. B. Ma, D. X. Dai, H. J. Fan, T. K. Minton, and X. M. Yang, J. Am. Chem. Soc. **134**, 13366 (2012).
[11] D. Wei, X. C. Jin, C. Q. Huang, D. X. Dai, Z. B. Ma, W. X. Li, and X. M. Yang, J. Phys. Chem. C **119**, 17748 (2015).
[12] M. M. Shen and M. A. Henderson, J. Phys. Chem. Lett. **2**, 2707 (2011).
[13] X. C. Mao, Z. Q. Wang, X. Lang, Q. Q. Hao, B. Wen, D. X. Dai, C. Y. Zhou, L. M. Liu, and X. M. Yang, J. Phys. Chem. C **119**, 6121 (2015).
[14] P. Biloen and W. M. Sachtler, Adv. Catal. **30**, 165 (1981).
[15] J. Zhu, J. Catal. **225**, 388 (2004).
[16] H. Idriss, K. S. Kim, and M. A. Barteau, Surf. Sci. **262**, 113 (1992).
[17] C. B. Xu, W. S. Yang, Q. Guo, D. X. Dai, T. K. Minton, and X. M. Yang, J. Phys. Chem. Lett. **4**, 2668 (2013).
[18] T. Cremer, S. C. Jensen, and C. M. Friend, J. Phys. Chem. C **118**, 29242 (2014).

DOI:10.1063/1674-0068/31/cjcp1806137

[19] Q. Yuan, Z. F. Wu, Y. K. Jin, F. Xiong, and W. X. Huang, J. Phys. Chem. C **118**, 20420 (2014).
[20] Z. R. Zhang, M. R. Tang, Z. T. Wang, Z. Ke, Y. B. Xia, K. T. Park, I. Lyubinetsky, Z. Dohnlek, and Q. F. Ge, Top. Catal. **58**, 103 (2014).
[21] K. Zhu, Y. B. Xia, M. R. Tang, Z. T. Wang, B. Jan, I. Lyubinetsky, Q. F. Ge, Z. Dohnálek, K. T. Park, and Z. R. Zhang, J. Phys. Chem. C **119**, 14267 (2015).
[22] K. Zhu, Y. B. Xia, M. R. Tang, Z. T. Wang, I. Lyubinetsky, Q. F. Ge, Z. Dohnálek, K. T. Park, and Z. R. Zhang, J. Phys. Chem. C **119**, 18452 (2015).
[23] H. Feng, L. M. Liu, S. H. Dong, X. F. Cui, J. Zhao, and B. Wang, J. Phys. Chem. C **120**, 24287 (2016).
[24] L. M. Liu and J. Zhao, Surf. Sci. **652**, 156 (2016).
[25] X. J. Yu, Z. R. Zhang, C. W. Yang, F. Bebensee, S. Heissler, A. Nefedov, M. R. Tang, Q. F. Ge, L. Chen, B. D. Kay, Z. Dohnálek, Y. M. Wang, and C. Wöll, J. Phys. Chem. C **120**, 12626 (2016).
[26] D. W. Guan, R. M. Wang, X. C. Jin, D. X. Dai, Z. B. Ma, H. J. Fan, and X. M. Yang, Chin. J. Chem. Phys. **30**, 253 (2017).
[27] B. Luo, H. Q. Tang, Z. W. Cheng, Y. Y. Ji, X. F. Cui, Y. L. Shi, and B. Wang, J. Phys. Chem. C **121**, 17289 (2017).
[28] M. Setvin, J. Hulva, H. H. Wang, T. Simschitz, M. Schmid, G. S. Parkinson, C. Di Valentin, A. Selloni, and U. Diebold, J. Phys. Chem. C **121**, 8914 (2017).
[29] Z. M. Wang, F. Xiong, Z. Zhang, G. H. Sun, H. Xu, P. Chai, and W. X. Huang, J. Phys. Chem. C **121**, 25921 (2017).
[30] H. Qiu, H. Idriss, Y. Wang, and C. Wöll, J. Phys. Chem. C **112**, 9828 (2008).
[31] Q. Yuan, Z. F. Wu, Y. K. Jin, L. Xu, F. Xiong, Y. Ma, and W. X. Huang, J. Am. Chem. Soc. **135**, 5212 (2013).
[32] M. A. Henderson, Surf. Sci. **319**, 315 (1994).
[33] M. A. Henderson, Langmuir **12**, 5093 (1996).
[34] T. L. Thompson, O. Diwald, and J. T. Yates, J. Phys. Chem. B **107**, 11700 (2003).
[35] M. A. Henderson, N. A. Deskins, R. T. Zehr, and M. Dupuis, J. Catal. **279**, 205 (2011).
[36] M. A. Henderson, J. Phys. Chem. **99**, 15253 (1995).
[37] R. Atkinson, D. L. Baulch, R. A. Cox, J. N. Crowley, R. F. Hampson, R. G. G. Hynes, M. E. Jenkin, M. J. Rossi, and J. Troe, Atmos. Chem. Phys. **6**, 3625 (2006).
[38] R. T. Zehr and M. A. Henderson, Surf. Sci. **602**, 1507 (2008).
[39] X. C. Mao, D. Wei, Z. Q. Wang, X. C. Jin, Q. Q. Hao, Z. F. Ren, D. X. Dai, Z. B. Ma, C. Y. Zhou, and X. M. Yang, J. Phys. Chem. C **119**, 1170 (2014).

Qing Guo received his B.S. degree in Chemical Physics from University of Science and Technology of China (USTC) in 2007, and Ph.D. from State Key Laboratory of Molecular Reaction Dynamics, Dalian Institute of Chemical Physics, Chinese Academy of Sciences (CAS) in 2013 under the supervision of Prof. Xue-ming Yang. He is now an associate professor at the State Key Laboratory of Molecular Reaction Dynamics, Dalian Institute of Chemical Physics, CAS. His current research is focused on the dynamic and mechanistic aspects of photocatalytic reactions on model semiconductor photocatalysts.

DOI:10.1063/1674-0068/31/cjcp1806137